

Magnetic Freezeout and Band Tailing in n -InAs

L. A. Kaufman*

Department of Physics, Tufts University, Medford, Massachusetts 02155 and

Francis Bitter National Magnet Laboratory, † Massachusetts Institute of Technology, Cambridge, Massachusetts 02139

and

L. J. Neuringer

Francis Bitter National Magnet Laboratory, † Massachusetts Institute of Technology, Cambridge, Massachusetts 02139

(Received 1 April 1970)

The temperature and magnetic field dependence of the Hall coefficient of n -InAs have been measured in static magnetic fields up to 210 kG over the interval 0.5–4.2 K. We have observed magnetic freezeout in three samples with excess donor concentrations $(N_D - N_A) = 9.5 \times 10^{15}$, 1.1×10^{16} , and $1.8 \times 10^{16} \text{ cm}^{-3}$. A new result of these experiments is the evidence that Gaussian-like tails are present on the densities of states of the conduction band and impurity level. These tails are due to random fluctuations in the impurity density. The extent of this band tailing was determined from the experimental data and the theory of Dyakonov, Efros, and Mitchell. However, to explain the observed activation energy and its temperature dependence it was necessary to develop a model based on the existence of localized states deep in the conduction-band tail.

I. INTRODUCTION

In n -type InAs all of the electrons in the conduction band occupy the $n=0$ Landau level when the quantum limit is attained, i. e., $\omega_c \tau \gg 1$ and $\hbar\omega_c > \mathcal{E}$, where $\omega_c = eH/m^*c$ is the cyclotron frequency and \mathcal{E} is the energy of a typical electron. Under these conditions a further increase of the magnetic field intensity H will affect the equilibrium population of the electrons in the conduction band n_c . The intense magnetic field shrinks the electronic wave function into a volume which is comparable to, or less than, the average volume occupied by an impurity ion. As a result a bound state is formed, due to the presence of the magnetic field, and the binding energy $\epsilon_b(H)$ of this state increases as H becomes greater. Charge carriers will then freeze out of the $n=0$ level and onto the impurity bound states if $\epsilon_b(H) > kT$. The electrons will become localized about impurity ions and the ratio n_c/N_0 becomes less than unity, where $N_0 = (N_D - N_A)$ is the excess concentration of donor ions. At fixed temperature this magnetic freezeout phenomenon is observed as an increase in the Hall coefficient $R(H)$ with magnetic field. In particular $R(H)$ has been found^{1,2} to vary as $R(H) \propto \exp[\epsilon_b(H)/kT]$ in n -InSb when $1.5 \leq T \leq 4.2$ K.

In the present work we report on the temperature and magnetic field dependence of $R(H)$ in the freezeout regime for samples of n -InAs. A new result of these experiments is the evidence that Gaussian-like tails are present on the densities of states of the conduction band and impurity level. These tails are due to random fluctuations in the impurity

density. It is found for n -InAs that, whereas the magnetic field dependence of $\epsilon_b(H)$ is given by $\epsilon_b \propto H^{1/3}$, in agreement with the previous experimental work^{1,2} on n -InSb, the magnitude of ϵ_b in the present work is considerably less than theoretical estimates³⁻⁶ of the binding energy. Furthermore, in the present experiments the ratio $\epsilon_b/kT \geq 25$, thereby indicating that n_c/N_0 , which varies as $\exp(-\epsilon_b/kT)$, should be very small; but we observe that during freezeout the decrease in n_c/N_0 is less than one order of magnitude. More significantly, in the freezeout domain at fixed H , we find that as a function of temperature n_c/N_0 decreases initially but approaches a constant value at the lowest temperatures. These results cannot be understood solely in terms of a model³⁻⁶ which assumes an unbroadened impurity level moving away with increasing H from a sharply defined conduction-band edge. For example, according to such a model one expects $n_c/N_0 \rightarrow 0$ as $T \rightarrow 0$, but this is contrary to our observations.

To explain the data, it is necessary to include in the theory the effect of spatial fluctuations in the random distribution of impurity ions. If in some small region there exists a locally higher-than-average impurity concentration, there will be a local lowering of the potential and vice versa. The effect of such a fluctuation potential has been investigated theoretically⁷⁻¹⁰ for $H=0$ and it was found to introduce a tail on the conduction-band density of states and to broaden the impurity level. These results have recently been extended by Dyakonov, Efros, and Mitchell¹¹ (hereafter DEM) to

TABLE I. Properties of *n*-InAs samples at 77 K.

Sample No.	Excess donor concentration $N_0 = (N_D - N_A)$ (cm^{-3})	Hall mobility μ_H ($\text{cm}^2/\text{V sec}$)
915	9.5×10^{15}	7.1×10^4
116	1.1×10^{16}	6.0×10^4
216	1.8×10^{16}	4.4×10^4

the case of a highly compensated semiconductor subject to magnetic fields corresponding to those necessary for carrier freezeout. We discuss the temperature and magnetic field dependence of the Hall coefficient by making use of the densities of states as calculated by DEM, and deduce quantitative estimates of the extent of band tailing in *n*-InAs. Furthermore, level broadening causes overlap of the conduction band and impurity level at all experimental magnetic field intensities. This situation would normally exclude the possibility of an activation energy, contrary to our observations. We have therefore developed a model which accounts in a consistent manner for the experimentally measured activation energy in the freezeout regime.

II. EXPERIMENT

Measurements of the temperature and magnetic field variation of the Hall coefficient were made in samples of *n*-type InAs over the range 0.5–4.2 K in static magnetic fields up to 210 kG. The bridge-shaped single-crystal samples were obtained from the Bell and Howell Company and are of good quality, as evidenced by their mobility. The electrical properties of these samples at 77 K are listed in Table I. They possess the smallest charge carrier concentration of any samples we have obtained. The samples were not intentionally counterdoped during synthesis and, whereas their compensation ratio $K = N_A/N_D$ is not known, it is reasonable to expect a value on the order of $K \leq 0.5$. Electrical contacts to the samples were made with pure indium and were checked for Ohmic behavior. The measurements were performed with a dc technique and great care was taken to limit the current through the sample to avoid self-heating effects.

Temperatures below 1 K were achieved and maintained with a recirculating refrigerator by pumping over a liquid He³ bath. The temperature of the samples at $T < 1.2$ K was determined from the vapor pressure of He³ condensed in a separate bulb to which the sample was thermally anchored. The vapor pressure of a He⁴ bath was used to determine the temperature when operating above 1.2 K.

III. RESULTS

Representative experimental results of the Hall

coefficient for sample No. 116 are shown in Fig. 1, where $R(H)$ is plotted semilogarithmically as a function of $H^{1/3}$. At low and moderate fields, $R(H)$ is practically independent of the magnetic field. At these field values, the electronic wave functions on adjacent impurities overlap sufficiently to cause the impurity level to merge with the conduction band. As the magnetic field is increased the electronic wave functions are reduced in size, thus reducing the amount of wave-function overlap. Wave-function overlap is relatively unimportant once the magnetic field shrinks the electronic wave-function volume to a value on the order of, or less than, the average impurity volume N_0^{-1} . The donor ions are then de-ionized and $R(H)$ increases, as evidenced by the linear portions of the curves in Fig. 1. For magnetic fields within the $\epsilon_b \propto H^{1/3}$ domain, we also observe¹² an increase of the transverse magnetoresistance $\rho_L(H)$ with increasing H or decreasing temperature. Both the magnetoresistance and Hall coefficient measurements indicate that the conduction band becomes progressively depopulated and that there exists an activation energy which increases as H increases. Details concerning the

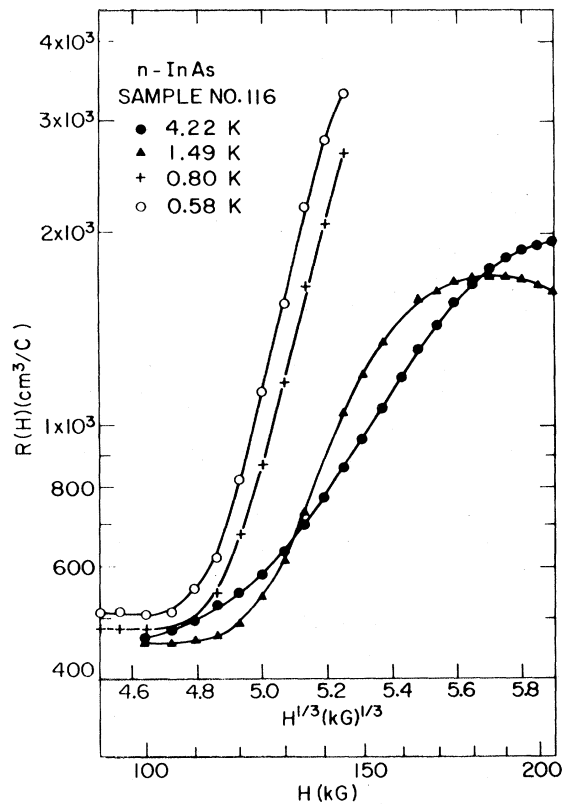


FIG. 1. Magnetic field dependence of the Hall coefficient of *n*-type InAs at several temperatures, $(N_D - N_A) = 1.1 \times 10^{16} \text{ cm}^{-3}$.

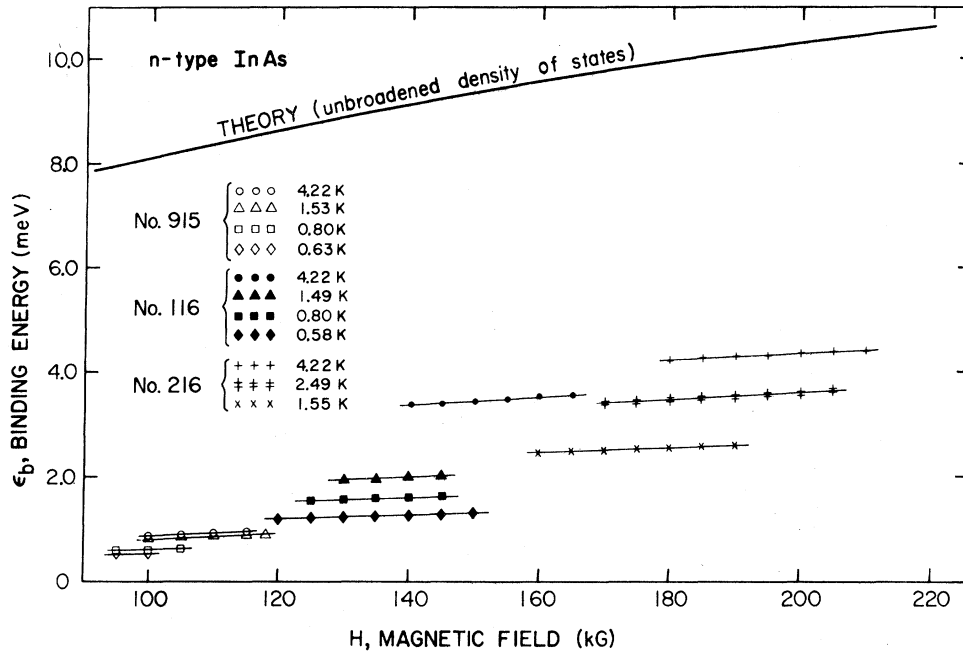


FIG. 2. Comparison of theory and experiment for the binding energy of the magnetic-field-induced bound state.

magnetoresistance measurements on these samples will appear in a forthcoming paper.

Experimental values of ϵ_b deduced from the slopes of $\ln R(H)$ -versus- $H^{1/3}$ curves at various fixed temperatures are shown in Fig. 2. It should be noted that these results have been obtained within the framework of a single-band conduction model. We have no evidence that multiband conduction is important in these samples. In fact, we found that $\rho_L(H)$ is independent of magnetic field at the highest magnetic fields and lowest temperatures, where impurity level conduction would be expected to dominate. If impurity conduction were important, $\rho_L(H)$ should increase rapidly with increasing H due to the reduction of the impurity band mobility. This is not observed, and it is concluded that single-band conduction is a proper description of the experimental results in the freezeout regime. The solid line in Fig. 2 is the theoretical curve derived from a variational calculation of the binding energy due to Larsen.³ This calculation does not include the effect of level broadening arising from impurity density fluctuations. The experimental data obey an $\epsilon_b \propto H^{1/3}$ relationship, but the magnitude of ϵ_b is significantly less than predicted by the theory. In addition, ϵ_b is seen to be temperature dependent, decreasing as the temperature decreases.

The temperature variation of $-\ln(n_c/N_0)$ at fixed magnetic field is shown in Fig. 3 for sample Nos. 915 and 116. The magnetic fields at which these data are plotted lie well within the domain where $\epsilon_b \propto H^{1/3}$. Hence, any temperature variation of

$-\ln(n_c/N_0)$ must be attributed to depopulation of the conduction-band states. The data in Fig. 3 exhibit a feature which has not been observed heretofore in experiments on magnetic freezeout. One would expect that these curves should be straight lines with slope ϵ_b/k as the temperature is progressively lowered at fixed H and n_c decreases due to carrier freezeout effects. Instead, there is observed an approach to a constant value at the lowest temperatures, which indicates that the Fermi level remains in, or very near to, the conduction band at these lowest temperatures.

IV. ANALYSIS

The measurements of the Hall coefficient as a function of temperature and magnetic field have revealed (i) that the concentration n_c approaches a constant value as $T \rightarrow 0$, (ii) a significant difference between the experimental binding energy and the value calculated from Larsen's theory, and (iii) a temperature variation of the binding energy, the binding energy decreasing with decreasing temperature. These results can be explained within a framework wherein the effect of spatial fluctuations in the impurity density are taken into account.

A. Density-Fluctuation Model

In the model which describes the fluctuation effects, one considers a volume $\frac{4}{3}\pi r_s^3$, where r_s is a screening length. A particular volume will contain some number of impurity ions. Due to the random distribution of ions in the crystal, there will be a fi-

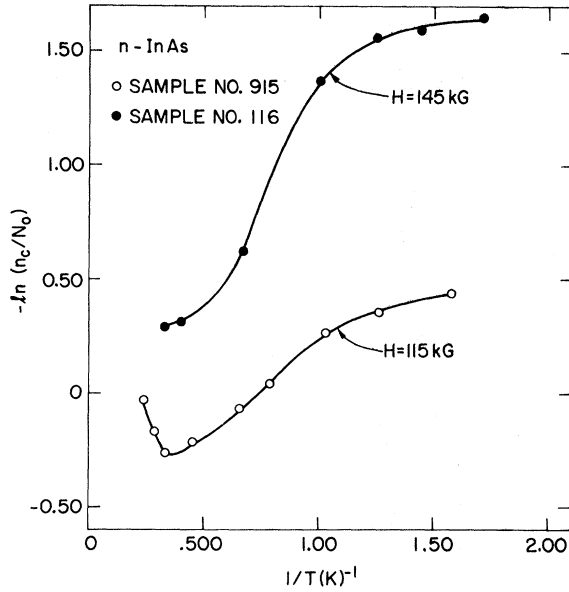


FIG. 3. Temperature dependence of conduction-band carrier concentration, at fixed H in the freezeout regime, for two samples of n -type InAs with $(N_D - N_A) = 9.5 \times 10^{15} \text{ cm}^{-3}$ and $1.1 \times 10^{16} \text{ cm}^{-3}$.

nite probability that within one such volume the number of ions may be more or less than the average number. Since the crystal is comprised of many such volumes, spatial density fluctuations will exist. These spatial fluctuations cause fluctuations in the potential energy of the electrons. If the average number of impurity ions within one volume is large enough, then the potential is slowly varying and can be taken as approximately constant within this volume. A local density of states can then be defined for this volume, and this local density of states changes from volume to volume, reflecting the fluctuations in the spatial density of impurity ions. The full density of states is derived by taking the average of the local density over a potential distribution function. A Gaussian distribution function is found for the fluctuating potential provided the average number of ions within the volume is very large. This results, after averaging, in a Gaussian-like broadening of the full density of states of the conduction band and impurity level. The parameter which characterizes the magnitude of this broadening corresponds physically to the average value of the fluctuation potential and is given by^{9,11}

$$\Gamma = 2\pi^{1/2} (e^2/\kappa r_s) (N r_s^3)^{1/2}, \quad (1)$$

where $N = (N_D + N_A)$ and κ is the static dielectric constant.

The density of states $g(x)$ is plotted in the quantum limit in Fig. 4 for a semiconductor containing

donor impurities. In this figure the energy ϵ is normalized to the value of Γ . Figure 4(a) is a diagram of the unbroadened densities of states of n -InAs calculated at $H = 145 \text{ kG}$. The zero of energy is taken at the bottom of the unbroadened $n = 0$ Landau level. The binding energy ϵ_b , predicted by the theory³ which neglects fluctuation effects corresponds in Fig. 4(a) to the energy difference between the well-defined impurity level and the sharp conduction-band edge. In contrast to this situation, Fig. 4(b) displays the conduction-band and impurity-level densities of states as calculated from the DEM model using the expressions

$$g_c(x) = \frac{m^{1/2} eH}{2^{3/2} \pi^{5/2} \hbar^2 c \Gamma^{1/2}} \int_{-\infty}^x dy \frac{\exp(-y^2)}{(x-y)^{1/2}} \quad (2)$$

and

$$g_i(x) = (N_D/\pi^{1/2}\Gamma) \exp[-(x+x_b)^2], \quad (3)$$

where $g_c(x)$ and $g_i(x)$ are the conduction-band and impurity-level state densities, respectively, m is an effective mass, taken here to be the cyclotron mass $m^* = 0.022m_0$, and $x_b = \epsilon_b/\Gamma$. The densities of states depend explicitly on H and Γ , and the

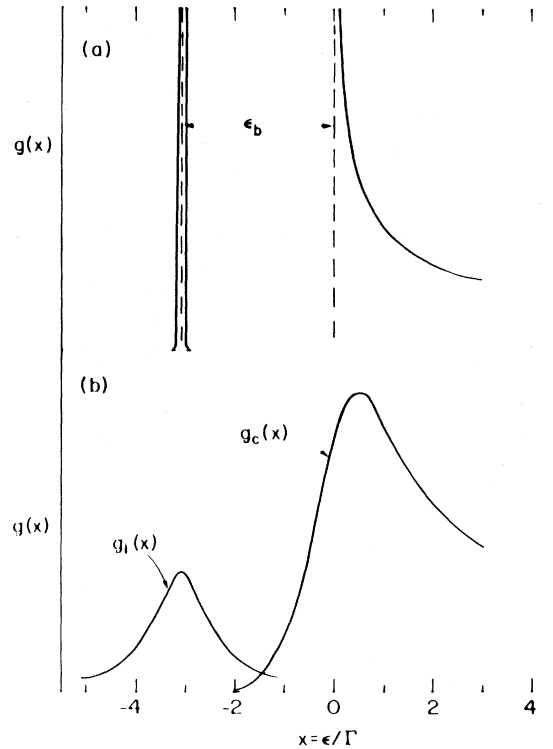


FIG. 4. Plot of the densities of states in the quantum limit for n -type InAs, with shallow donor impurities. In (a) the idealized case of no broadening is depicted. The broadened density of states derived from the DEM theory with $\Gamma = 3 \text{ meV}$ is shown in (b). Both cases are shown for $H = 145 \text{ kG}$.

curves in Fig. 4(b) are calculated for $H = 145$ kG and $\Gamma = 3$ meV. It should be noted that at fixed H and Γ , the asymptotic expression for $g_c(x)$, valid for $x < 0$ and $|x| \gg 1$, is given by

$$g_c(x) = (\text{const}) |x|^{-1/2} \exp(-x^2). \quad (4)$$

Equations (3) and (4) exhibit the Gaussian-like properties of $g_i(x)$ and $g_c(x)$, and show that Γ is a measure of the broadening of the impurity level and the extent of the tail on the conduction band.

Using the densities of states as given by Eqs. (2) and (3) it is now possible to discuss within this model the temperature and magnetic field dependence of n_c in the freezeout regime. DEM have shown¹³ that

$$n_c = n_0 \exp \left[-\frac{\epsilon_b}{kT} - \frac{\chi\Gamma}{kT} + \left(\frac{\Gamma}{2kT} \right)^2 \right], \quad (5a)$$

where $n_0 = (2\pi)^{1/2} eH(mT)^{1/2}/h^2c$ and χ is a constant which is zero for samples in which $K \leq 0.5$. Even though χ is finite for $K > 0.5$, it is still small compared to other terms in Eq. (5a). For the present experiments, therefore, we may write

$$n_c = n_0 \exp \left[-\frac{\epsilon_b}{kT} + \left(\frac{\Gamma}{2kT} \right)^2 \right]. \quad (5b)$$

Equation (5b) is strictly valid in the limit of nondegenerate electron statistics. An analysis of the transverse magnetoresistance data¹² for these samples indicates that the electrons are in or near the nondegenerate limit at low temperatures. This analysis supports the argument that at intense magnetic fields, $H \approx 150$ kG, all of the conduction-band electrons can be accommodated in the tail ($x < 0$) of the conduction band. The number of available states in the tail is given approximately by $(2m)^{1/2} eH\Gamma^{1/2}/h^2c \approx 3 \times 10^{16} \text{ cm}^{-3}$ which is greater than N_0 for these samples. In addition, magnetically bound states exist and are occupied at this field intensity. Therefore, the Fermi level is located deep in the tail of the conduction band and will correspond to a nondegenerate distribution as will be shown in our discussion of the binding energy.

B. Extent of Level Broadening

We now discuss the extent of the level broadening as measured by the parameter Γ . Our objective is to deduce experimental values of Γ and to compare them with the predictions of Eq. (1). The experimental values of Γ are derived in the freezeout regime from Eq. (5b) at various temperatures for fixed H . These values are listed in the third column of Table II. When calculating Γ from Eq. (1), one is faced with the problem of the choice of an appropriate screening radius r_s . In the work of DEM it was assumed that r_s is an ionic screening

radius corresponding to a Debye-Huckel correlation length¹⁴ which is frozen in when the crystal solidifies. The temperature at which this screening length r_s is calculated corresponds approximately to the crystallization temperature. This screening length is the important one provided the electronic screening radius $\lambda_s > r_s$. This is not the case in the present experiments because $\lambda_s < r_s$. One should also be aware that, in practice, there are difficulties in calculating an electronic screening radius, as has been pointed out.¹⁵ To be consistent with the previous discussion on carrier statistics, we take $\lambda_s^2 = \kappa kT/4\pi e^2 n_c$ which is the nondegenerate screening length. The carrier concentration used in this formula must reflect the fact that λ_s depends on the magnetic field and temperature since n_c is changing during the freezeout process. The values of Γ predicted by Eq. (1), and listed in the last column of Table II, were calculated using λ_s , the nondegenerate screening length given above. As a result, Γ should become temperature and magnetic field dependent through T/n_c , although in practice it is found that the magnetic field dependence is weak.

A comparison between the experimental values of Γ and the theoretical values estimated from Eq. (1) is given in Table II at the highest and lowest temperatures studied for each sample. It is found that for a given sample Γ (expt) decreases monotonically as the temperature is lowered. In relatively uncompensated samples, for which $\lambda_s < r_s$, this is just the type of behavior expected because $\Gamma \propto \lambda_s^{1/2}$ and λ_s decreases as T decreases. It is significant that on this basis Γ would be independent of temperature for a strongly degenerate electronic distribution. Hence, the temperature dependence of Γ is taken as further evidence of the electronic distribution being near to, or in, the nondegenerate limit. From the results in Table II, one may be tempted to draw the additional conclusion that Γ (expt) is an increasing function of the impurity concentration. Although this conclusion is consistent with Eq. (1), the differences of Γ among the samples are not judged to be significant in light of the various approximations which were made. There is good agreement between the values

TABLE II. Values of Γ in the nondegenerate limit.

Sample No.	T (K)	Γ (expt) (meV)	Γ (theor) (meV)
915	4.2	3.5	3.0
	0.63	1.4	2.1
116	4.2	3.6	3.5
	0.58	1.4	3.0
216	4.2	3.8	3.9
	1.55	2.3	3.0

of Γ in Table II at the higher temperatures, but a discrepancy is evident at the lower temperatures. A possible origin of this discrepancy can be traced to our incomplete knowledge of the correct screening length when calculating Γ (theor). At the lowest temperatures where a majority of the conduction electrons are frozen out, screening contributions from the bound electrons become important. Kane has indicated⁹ that the screening length due to the bound electrons at $H=0$ is approximately one-half of the effective Bohr radius for the bound electron. A quantitative estimate of this effect is difficult because of the complications introduced by the fluctuation broadening of the bound electron states. Nevertheless, if the contribution to the screening by the bound electrons is included, it will reduce the value of Γ (theor) at the lowest temperature and would improve agreement with experiment.

Preliminary results on carrier freezeout experiments in n -InSb indicate that densities-of-states broadening also plays a role in this material. The experimental value of Γ in InSb is about 0.7 meV at 0.8 K for a sample with $N_0 = 2 \times 10^{15} \text{ cm}^{-3}$. The effect of broadening on the thermal activation energy of this sample was not observed above 1 K because $\epsilon_b/kT > \Gamma^2/(2kT)^2$ at these temperatures.

C. Activation Energy

In the preceding sections we have discussed a distinctive feature of these experiments, namely, the presence of band tailing and broadening. This feature will modify the characteristics of the magnetic freezeout. In particular, overlap of the conduction-band tail and impurity level exists at all values of the magnetic field and temperature investigated. This overlap would normally exclude the possibility of an activation energy whereas, in fact, we observe one. Moreover, the observed values of ϵ_b are appreciably smaller than predicted by the currently available theories³⁻⁶ and ϵ_b decreases as T is lowered. These experimental observations necessitate a discussion of the origin of the activation energy.

Referring to Fig. 5, where $g_i(x)$ and $g_c(x)$ are plotted versus x , one notices that the Fermi distribution function edge is sharp relative to x since in our experiments $kT \leq 3 \times 10^{-4} \text{ eV}$. Because the samples are compensated, the Fermi level is located on the impurity level and its exact position is governed by the degree of compensation K . Due to the compensation and to the sharpness of the distribution, the Fermi level represents the demarcation between filled and empty states in the impurity level. If $K \leq 0.5$, then at low temperatures, the reduced Fermi level $\eta = E_f/\Gamma$ will be located approximately as shown in Fig. 5 where the

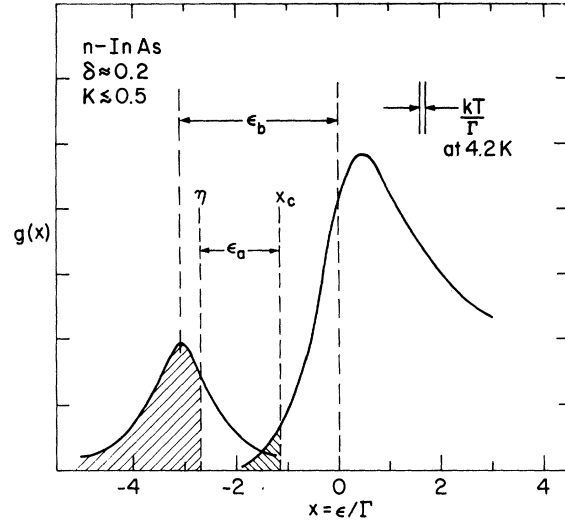


FIG. 5. Broadened density of states for n -type InAs at $H=145 \text{ kG}$, $\Gamma=3 \text{ meV}$. The experimental activation energy according to our model is denoted by ϵ_a , where $\delta \approx 0.2$ and $K \lesssim 0.5$. The shaded portions under the densities-of-states curves represent electronic states which do not contribute to the conduction process.

filled impurity states lying below η are shaded.

We now examine the electronic states in the conduction-band tail. The states in this tail correspond to electrons in real space localized within a volume of the order of λ_s^3 . The theory¹¹ describes the random potential in terms of a single λ_s . Smaller volumes λ_s^3 give rise to larger statistical fluctuations in the potential. Hence, the smaller values of λ_s are increasingly important to the determination of $g_c(x)$ for states deep in the tail. As a result, the deeper one proceeds into the conduction-band tail, the more localized the electrons become in real space. According to this model there should exist an energy E_c which corresponds to the transition between the localized and nonlocalized states. In fact, Mott^{16,17} has suggested that the Anderson¹⁸ criterion for localization is applicable to states in the conduction-band tail arising from density fluctuations. For states deep in the tail, localization occurs in the sense that these states do not contribute to conduction. The reduced energy $x_c = E_c/\Gamma$ is shown in Fig. 5 and the localized conduction-band states lying below x_c are shaded. We can locate the position of x_c approximately if we follow Mott's suggestion¹⁷ that localized states occur when the ratio δ of the perturbed (due to density fluctuations) density of states to the unperturbed value falls to $\approx 0.2-0.5$. This is shown in Fig. 5 where x_c occurs at a value corresponding to 0.2 of the unperturbed $g_c(x)$ value.

We are now in a position to understand the vari-

ous details of the activation energies. We denote, in Fig. 5, the experimentally observed activation energy by ϵ_a and the unbroadened theoretical³⁻⁶ value by ϵ_b , as in Fig. 4(a). Within this model the observed activation energy ϵ_a corresponds to the minimum energy required to excite an electron from the Fermi level at η to the nonlocalized states above x_c . It is seen that the activation energies ϵ_a deduced from this model are approximately one-half, or smaller, than those expected when level broadening and tailing are absent. This is, in fact, observed to occur as may be seen in Fig. 2. The position of x_c in Fig. 5, suggested by Mott's theory, leads to values of ϵ_a in agreement with those in Fig. 2. The reduced Fermi level η in this model lies deep in the conduction-band tail within the localized electronic levels. Thus, the Fermi level may be in the conduction-band tail, even though the carriers above x_c are nondegenerate. This is consistent with our earlier interpretation that the conduction electrons can be treated by nondegenerate statistics.

The temperature dependence of the experimentally observed activation energy is explained in the following manner. As the temperature is reduced in the freezeout regime, for fixed H , electrons fall into the impurity states. The Fermi level which is the demarcation between empty and full states in the impurity level shifts toward higher energies as the impurity level fills with electrons. Thus $\epsilon_a/\Gamma = (x_c - \eta)$ will decrease as T is lowered. This is the behavior that is observed experimentally, as is seen in Fig. 2.

We now consider the low-temperature behavior of $-\ln(n_c/N_0)$ in Fig. 3. The experimental values for ϵ_a satisfy the condition $\Gamma \gtrsim \epsilon_a$. As a direct consequence of this condition and because of the

presence of overlap, the Fermi level will remain sufficiently close to the nonlocalized states to allow for thermally activated carriers at the lowest temperatures. Thus, the magnitude of n_c will be comparable to N_0 and $-\ln(n_c/N_0)$ will approach a constant value at low temperatures, as in Fig. 3. The calculations of DEM carried out under the above conditions support this conclusion, namely, that $-\ln(n_c/N_0)$ approaches a constant value at low temperatures.

V. CONCLUSIONS

The results of our magnetic-freezeout experiments in n -InAs have indicated the presence of band tailing in the densities of states of the conduction band and impurity level. The extent of the band tailing is determined from the experimental data and the theory of DEM. A consistent interpretation of the results on the binding energy and its temperature dependence requires the hypothesis that electron states deep in the conduction-band tail do not contribute to the conduction. These electrons in the conduction-band-tail states represent electrons localized in real space in regions of the order of the screening length.

ACKNOWLEDGMENTS

It is a pleasure for us to acknowledge the warm and continuing relationship with Professor K. A. McCarthy. One of us (L. A. K.) is especially grateful for her guidance in his Ph.D. dissertation. This work could not have been possible without her continuing encouragement. In addition, we acknowledge helpful discussions with D. L. Mitchell, D. Adler, and L. G. Rubin. The technical support of B. Perry and V. Diorio is greatly appreciated.

*Work supported in part by National Science Foundation Grant No. GP-15993.

†Work supported by the U.S. Air Force Office of Scientific Research.

¹L. J. Neuringer, in *Proceedings of the Ninth International Conference on the Physics of Semiconductors*, edited by S. M. Ryvkin (Nauka Publishing House, Leningrad, 1968), Vol. 2, p. 715.

²O. Beckman, E. Hanamura, and L. J. Neuringer, *Phys. Rev. Letters* **18**, 773 (1967).

³D. M. Larsen, *J. Phys. Chem. Solids* **29**, 271 (1968).

⁴H. Hasegawa, *Physics of Solids in Intense Magnetic Fields* (Plenum, New York, 1969), Chap. 10, p. 246.

⁵R. J. Elliot and R. Loudon, *J. Phys. Chem. Solids* **15**, 196 (1960).

⁶Y. Yafet, R. W. Keyes, and E. N. Adams, *J. Phys. Chem. Solids* **1**, 137 (1956).

⁷B. I. Halperin and M. Lax, *Phys. Rev.* **148**, 722

(1966).

⁸T. N. Morgan, *Phys. Rev.* **139**, A343 (1965).

⁹E. O. Kane, *Phys. Rev.* **131**, 79 (1963).

¹⁰V. L. Bonch-Bruевич, *Fiz. Tverd. Tela* **4**, 2660 (1962) [*Soviet Phys. Solid State* **4**, 1953 (1963)].

¹¹M. I. Dyakonov, A. L. Efros, and D. L. Mitchell, *Phys. Rev.* **180**, 813 (1969).

¹²L. A. Kaufman and L. J. Neuringer (unpublished).

¹³The steps leading to the derivation of Eq. (5a) from the complete expression for n_c in the paper by DEM are not clear.

¹⁴L. V. Keldysh and G. P. Proshko, *Fiz. Tverd. Tela* **5**, 3378 (1963) [*Soviet Phys. Solid State* **5**, 2481 (1964)].

¹⁵D. Redfield and M. A. Afrimowitz, *Phil. Mag.* **19**, 831 (1969).

¹⁶N. F. Mott, *Advan. Phys.* **16**, 49 (1967).

¹⁷N. F. Mott, *Phil. Mag.* **19**, 835 (1969).

¹⁸P. W. Anderson, *Phys. Rev.* **109**, 1492 (1958).